OXFORD

Briefings in Bioinformatics, 2024, **25(2)**, 1–13
https://doi.org/10.1093/bib/bbae023
Case Study

Genomic hallmarks and therapeutic targets of ribosome biogenesis in cancer

Yue Zang[†], Xia Ran[†], Jie Yuan, Hao Wu, Youya Wang, He Li, Huajing Teng and Zhongsheng Sun

Corresponding authors. Zhongsheng Sun, HIM-BGI Omics Center, Hangzhou Institute of Medicine (HIM), Chinese Academy of Sciences, Hangzhou, China. Tel.: +86-571-88122266; E-mail: sunzs@biols.ac.cn; Huajing Teng, Department of Radiation Oncology, Peking University Cancer Hospital and Institute, Beijing 100142, China. Tel.: +86-10-88196505; E-mail: hjteng@bjmu.edu.cn

[†]Yue Zang and Xia Ran contributed equally to this work.

Abstract

Hyperactive ribosome biogenesis (RiboSis) fuels unrestricted cell proliferation, whereas genomic hallmarks and therapeutic targets of RiboSis in cancers remain elusive, and efficient approaches to quantify RiboSis activity are still limited. Here, we have established an in silico approach to conveniently score RiboSis activity based on individual transcriptome data. By employing this novel approach and RNA-seq data of 14 645 samples from TCGA/GTEx dataset and 917 294 single-cell expression profiles across 13 cancer types, we observed the elevated activity of RiboSis in malignant cells of various human cancers, and high risk of severe outcomes in patients with high RiboSis activity. Our mining of pan-cancer multi-omics data characterized numerous molecular alterations of RiboSis, and unveiled the predominant somatic alteration in RiboSis genes was copy number variation. A total of 128 RiboSis genes, including *EXOSC4*, *BOP1*, *RPLP0P6* and *UTP23*, were identified as potential therapeutic targets. Interestingly, we observed that the activity of RiboSis was associated with *TP53* mutations, and hyperactive RiboSis was associated with poor outcomes in lung cancer patients without *TP53* mutations, highlighting the importance of considering *TP53* mutations during therapy by impairing RiboSis. Moreover, we predicted 23 compounds, including methotrexate and CX-5461, associated with the expression signature of RiboSis genes. The current study generates a comprehensive blueprint of molecular alterations in RiboSis genes across cancers, which provides a valuable resource for RiboSis-based anti-tumor therapy.

Keywords: ribosome biogenesis; pan-cancer multi-omics; therapeutic target; drug response; impaired ribosome biogenesis checkpoint

INTRODUCTION

Ribosome biogenesis (RiboSis) is a complex process that generates ribosomes required for protein synthesis in the growth and proliferation of cells [1–3]. It is a tightly coordinated process that involves three RNA polymerases, approximately 80 ribosomal proteins, and approximately 200 non-ribosomal trans-acting factors [4, 5]. RiboSis includes rRNA transcription, rRNA cleavage, rRNA modification, ribosome assembly and export of ribosomal pre-particles [6]. In malignant cells, the genes involved in each substep of RiboSis undergo somatic alterations, resulting in ribosomopathies and an increased risk of carcinogenesis [7, 8]. The concept that 'ribosomes translate cancer' has gained increasing recognition [9, 10]. Thus, understanding the contribution of these alterations to pathogenesis will allow for unveiling novel and targetable vulnerabilities in cancer. Owing to large-scale and multi-dimensional open-access data, there are numerous pan-cancer studies relevant to gene signatures [11–16]. However, a systematic analysis of genes involved in RiboSis in human cancers has been lacking.

RiboSis initiates in the nucleolus and terminates in the cytoplasm [7]. Nucleolar size and density are highly dynamic and can be adjusted according to the demands of protein synthesis. Increasing evidence has underscored hyperactive RiboSis fuels unrestricted cell growth and proliferation, and it has emerged as a central player in cancer occurrence and metastasis [7, 17]. Aberrant increases in nucleolar size and number accommodated by dysregulation of RiboSis are regarded as hallmarks of the vast majority of cancers [18]. Silver staining of the argyrophilic nucleolar organizer region (AgNOR), where RiboSis takes place, is used as an indicator of cellular proliferative activity [19]. In addition, the expression of nucleolar protein fibrillarin [20, 21]

Yue Zang is a graduate student of HIM-BGI Omics Center, Hangzhou Institute of Medicine (HIM), Chinese Academy of Sciences and Institute of Genomic Medicine, Wenzhou Medical University, China. Her research interests include genomics and bioinformatics.
Xia Ran is a postdoctor of Liangzhu Laboratory, Zhejiang University Medical Center, China. Her research interests include genomics and bioinformatics.
Jie Yuan is a graduate student of BGI Education Center, University of Chinese Academy of Sciences, China. Her research interests include bioinformatics.
Hao Wu is a graduate student of Institute of Genomic Medicine, Wenzhou Medical University, China. Her research interests include genomics.
Youya Wang is a graduate student of Institute of Genomic Medicine, Wenzhou Medical University, China. Her research interests include genomics.
He Li is a graduate student of Institute of Genomic Medicine, Wenzhou Medical University, China. His research interests include bioinformatics.
Huajing Teng is an associate professor of Department of Radiation Oncology, Key Laboratory of Carcinogenesis and Translational Research (Ministry of Education) at Peking University Cancer Hospital and Institute. His research is in the areas of bioinformatics and genomics.
Zhongsheng Sun is a professor of HIM-BGI Omics Center, Hangzhou Institute of Medicine (HIM), Chinese Academy of Sciences, Institute of Genomic Medicine, Wenzhou Medical University, and Beijing Institutes of Life Science, Chinese Academy of Sciences. His research is in the areas of bioinformatics and genomics.
Received: October 26, 2023. **Revised:** January 11, 2024. **Accepted:** January 15, 2024

and the abundance of RNA polymerase I transcription factor [22] are commonly used to reflect the activity of RiboSis. Unfortunately, these experimental approaches are not suitable for some cancer types, particularly melanoma or mesothelioma [23] or are difficult to perform [24]. Several computational approaches have been developed to quantify biologically relevant activities between groups or samples based on gene set or signature scoring [25, 26]. However, there is still a lack of computational approach to efficiently and specifically quantify RiboSis activity in cancer.

The dysregulation of RiboSis in the proliferation of cancer cells provides targetable vulnerabilities for cancer therapy [27]. Several chemotherapeutic or targeted drugs, 5-fluorouracil, cisplatin, oxaliplatin, actinomycin D and poly-ADP ribose polymerase (PARP) inhibitors, have been proven to act through perturbation of RiboSis including inhibition of rRNA synthesis and rRNA processing [28–32]. Additionally, certain cancer therapies originally intended to kill cancer cells through inducing DNA damage actually impair RiboSis via multiple mechanisms [31]. Although a few anti-tumor drugs can inhibit ribosome biogenesis, these drugs mainly target the early substeps of RiboSis, such as rRNA transcription and pre-rRNA processing [33]. Among RiboSis-related genes, only *XPO1* and *MTOR* have been approved as drug targets in multiple myeloma and breast cancer. Thus, there is still much room for the development of anti-tumor drugs targeting RiboSis genes.

To determine genomic hallmarks and therapeutic targets of RiboSis in cancers, we first established an in silico approach to quantify the activity of RiboSis based on transcriptomic data for the first time. By employing this approach, RNA-seq data of 14 645 samples from TCGA/GTEx dataset and 917 294 single-cell expression profiles across 13 cancer types were analyzed, and RiboSis activity in human cancers and its clinical relevance were explored. The molecular alterations of RiboSis genes were further characterized, and potential therapeutic targets were identified based on the frequent alterations of RiboSis genes in malignant tumors.

MATERIALS AND METHODS

Evaluation of RiboSis activity

The gene set related to RiboSis was defined based on the GO term of the MSigDB and characterization of Nerurkar *et al.* [6], and the cancer genetic dependence of RiboSis genes was evaluated based on the genome-wide RNAi/CRISPR screening data of DepMap project. Inspired by the single sample gene set enrichment analysis method in the R package Gene Set Variation Analysis (GSVA) [25, 26], we developed a computational approach to systematically evaluate the RiboSis activity of each sample using the RiboSis gene set constructed above. More details about data collection and processing, evaluating RiboSis activity, receiver operating characteristics (ROC), and survival are available in the supplementary methods.

Characterization of RiboSis genomic hallmarks

The R package DESeq2 [34] was used to estimate differentially expressed RiboSis genes ($P_{adj} < 0.05$ and $|\log_2$ Fold Change$| > 1$). GISTIC2 [35] was used to evaluate focal somatic copy number alterations in RiboSis genes (q-value < 0.25 and confidence level > 99%). Enrichment analysis was performed separately in each cancer type ($P < 0.05$). More details about differential expression analysis, majority vote meta-analysis and characterization of recurrent copy number alterations are available in the supplementary methods.

Drug response analysis

The drug development level was defined based on information from the IDG program of the NIH. The R package oncoPredict (V0.2) [36] was used to predict drug sensitivity through machine learning methods. The Wilcoxon rank sum test was used to perform differential drug response analysis ($P_{adj} < 0.05$ and $|$effect size$| > 1$). More details about drug development level, drug response of patients and differential drug response analysis are available in the supplementary methods.

RESULTS

Systematic evaluation of ribosome biogenesis activity

To evaluate the demand for ribosomes in the proliferation of cancer cells, we developed an in silico approach to quantify RiboSis activity. First, we defined a RiboSis-related gene set including 331 genes according to GO term of MSigDB and the characterization of Nerurkar *et al.* [6] (Figure 1A; Supplementary Table S1, see available online at http://bib.oxfordjournals.org/). To characterize the cancer dependency of these RiboSis genes, we then analyzed the genome-wide screening data of CRISPR/RNAi in cancer cell lines from the DepMap [37]. A total of 251 (76%) RiboSis genes were defined as essential genes for tumor growth and survival (Figure 1B), and essential genes were significantly enriched in RiboSis genes compared to non-RiboSis genes (Figure 1B). Next, inspired by the single sample gene set enrichment analysis [26], we developed a novel in silico approach to calculate RiboSis activity (Figure 1C). In this method, multiple RiboSis genes, instead of a single RiboSis gene, were used and the background of non-RiboSis genes was considered, which ensured the robustness of the output data. Aberrant increases in the expression of the nucleolar fibrillarin are commonly used to reflect the upregulation of RiboSis [20, 38]. To evaluate the efficiency of our workflow, we analyzed the mRNA and protein expression data of 105 breast cancer samples from the TCGA-BRCA and CPTAC datasets. Significant associations were observed between the identified RiboSis activity and the expression of four available fibrillarin proteins including *RRP1*, *FBL*, *NOP56* and *USP36* (Figure 1D and E; Supplementary Figure S1, see supplementary data available online at http://bib.oxfordjournals.org/). Alterations in ribosome composition upon 5-fluorouracil treatment have been characterized, and 5-fluorouracil has robust RiboSis-inhibitory activity [27, 28, 39, 40]. To further explore the reliability of our approach, we analyzed alterations in single-cell RNA expression after 5-fluorouracil treatment [41]. RiboSis activity quantified by our approach was decreased following 5-fluorouracil treatment in colorectal cancer cells (Figure 1F). Together, these data suggest that our developed computational approach was reliable for evaluating ribosome biogenesis activity based on transcriptome expression data.

Hyperactive RiboSis activity in human cancers, especially in malignant cells

Using the above-developed approach, we analyzed the RNA-seq data of 14 645 samples from TCGA/GTEx datasets to evaluate RiboSis activity in 33 cancer types. RiboSis activity varied among different cancer types (Figure 2A). Lymphoid neoplasm diffuse large B-cell lymphoma (DLBC) had the highest, while kidney renal clear cell carcinoma (KIRC) had the lowest levels of RiboSis activity on average across all cancer types (Figure 2A), indicating the difference in demand for RiboSis in the proliferation of tumor cells

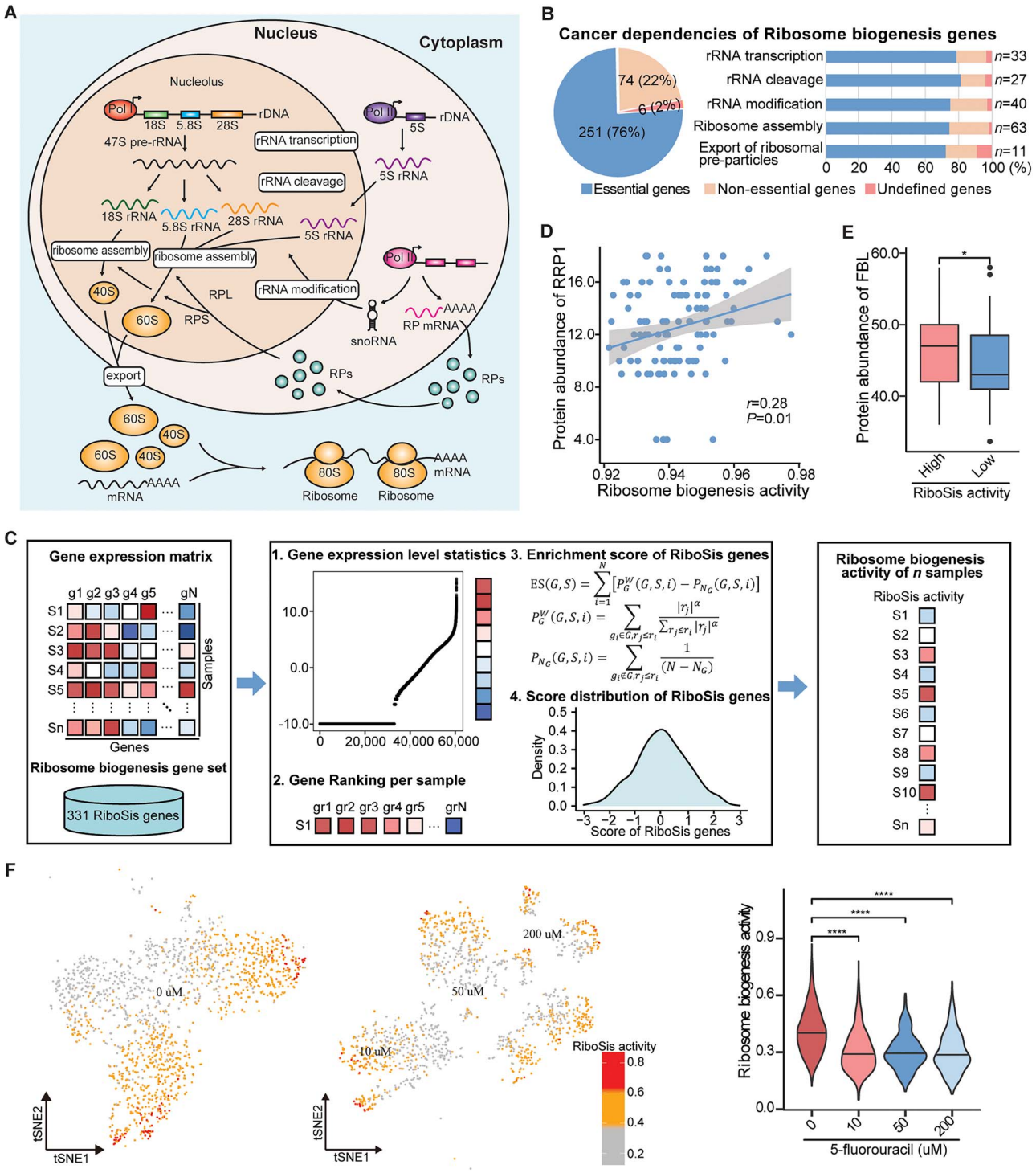

Figure 1. Development and validation of the approach to quantify ribosome biogenesis (RiboSis) activity. (**A**) Schematic of RiboSis in human cells adapted from [27]. rDNA: ribosomal DNA; rRNA: ribosomal RNA; RNA pol I/II/III: RNA polymerase I/II/III; snoRNA: small nucleolar RNA; RP: ribosome protein; RPS: ribosomal protein small subunits; RPL: ribosomal protein large subunits; 40S: small 40S ribosomal subunits; 60S: large 60S ribosomal subunits; 80S: mature 80S ribosome. (**B**) Summary of cancer dependencies of RiboSis genes. Left, the proportion of all 331 RiboSis genes that were essential genes, non-essential genes and undefined genes; Right, the proportion of RiboSis genes involved in each substep and the number of genes involved is marked on the right. (**C**) Workflow for evaluating RiboSis activity. The input includes the gene expression matrix and the RiboSis gene set, and the output is the RiboSis activity score of each sample. g: a specific gene; N: the total number of genes in the gene expression matrix; S: a specific sample; n: the total number of samples in the gene expression matrix; ES: enrichment score; G: the RiboSis gene set; r: the rank of a specific gene; N_G: the total number of RiboSis genes. A detailed description of this workflow is available in the supplementary methods. (**D**) The scatter diagram shows the correlation between RiboSis activity (calculated by the above workflow) and the protein abundance of RRP1 (obtained from CPTAC) in each patient with breast invasive carcinoma. (**E**) Boxplot showing the difference in the protein abundance of FBL between breast invasive carcinoma samples with high and low RiboSis activity. (**F**) tSNE representation (Left) and the difference (Right) in colorectal cancer cells' RiboSis activity after treatment with different doses of 5-fluorouracil. *$P < 0.05$ and ****$P < 0.0001$.

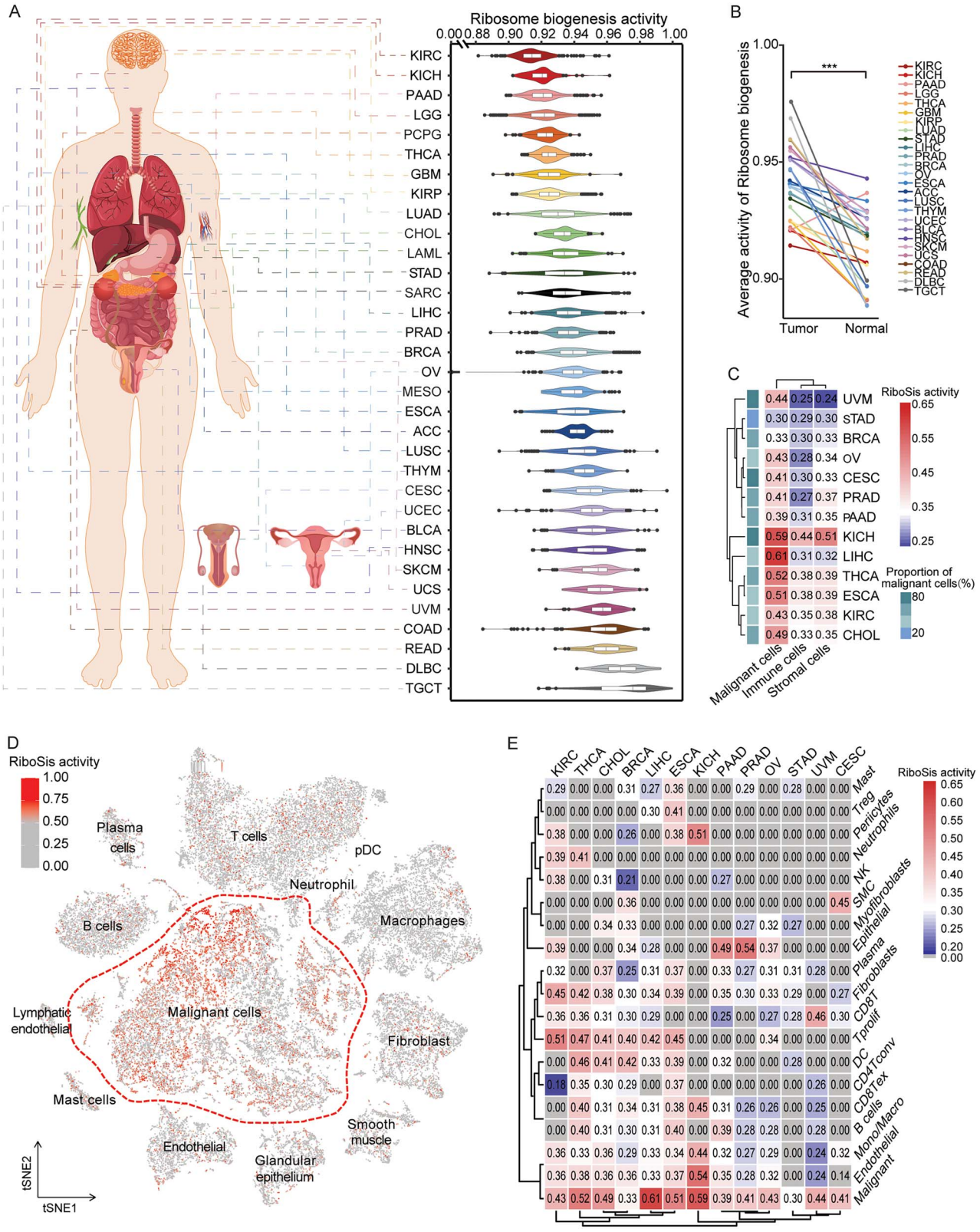

Figure 2. Hyperactive ribosome biogenesis (RiboSis) in human cancers. (**A**) Violin and boxplot showing RiboSis activity across 33 human cancer types. (**B**) The paired point plot shows the difference in the average activity of RiboSis between tumor and normal samples across 26 cancer types with a sufficient sample size. ***$P < 0.001$. (**C**) Heatmap showing RiboSis activity among malignant cells, immune cells and stromal cells across various human cancer types. (**D**) tSNE representation of RiboSis activity of different cell types in ESCC single-cell RNA-seq data. (**E**) Heatmap showing RiboSis activity among different cell subtypes across various human cancer types.

across various cancer types. In 25 of 26 cancer types with a sufficient sample size, RiboSis was significantly more active in tumors than normal tissues (Figure 2B; Supplementary Figure S2, see supplementary data available online at http://bib.oxfordjournals.org/), highlighting the importance of hyperactive RiboSis during tumorigenesis [27]. Furthermore, single-cell RNA-seq profiles of 13 cancer types were collected to evaluate RiboSis activity in different cell types besides malignant cells. Notably, RiboSis was more active in malignant cells than immune or stromal cells, and this phenomenon was irrelevant to the proportion of malignant cells (Figure 2C-E). Collectively, these data demonstrated that RiboSis was hyperactive in cancer, especially in malignant cells, providing the rationale for selectively targeting tumors over normal cells during anti-RiboSis therapy [42, 43].

Hyperactive RiboSis in cancer tissues inspired us to examine whether it could be used as a biomarker to distinguish cancer from normal tissues. Notably, RiboSis activity showed outstanding performance in distinguishing cancer tissues from normal tissues in 15 cancer types (Figure 3A; Supplementary Figure S3, see supplementary data available online at http://bib.oxfordjournals.org/). Then, we sought to explore whether it was correlated with patient prognosis in all of the 33 cancer types. We found that hyperactive RiboSis was a risk factor for poor clinical outcomes at the pan-cancer level (Figure 3B; Supplementary Figure S4, see supplementary data available online at http://bib.oxfordjournals.org/). Specifically, hyperactive RiboSis was associated with a poor progression-free interval in 15 cancer types including lung squamous cell carcinoma (LUSC), prostate adenocarcinoma (PRAD), head and neck squamous cell carcinoma (HNSC) and lung adenocarcinoma (LUAD) (Figure 3C). Collectively, RiboSis activity could serve as an effective biomarker for predicting cancer, and the risk of severe outcomes was increased in cancer patients with higher RiboSis activity.

RiboSis genes undergo high copy number amplification

To further determine the hallmarks of genomic alterations related to RiboSis, we first explored the expression signature of each RiboSis gene across human cancers and observed that upregulated RiboSis genes ($P_{adj} < 0.05$ and $|\log_2$ Fold Change$| > 1$) was significantly enriched in cancers (Figure 3D), highlighting the essential role of hyperactive RiboSis during tumorigenesis [27]. Notably, different types of cancer exhibit cancer-specific RiboSis gene dysregulation patterns (Figure 3E). Thus, we performed a majority vote meta-analysis of differentially expressed RiboSis genes across human cancers. Consistent with hyperactive RiboSis in cancers, 229 RiboSis genes (69%) were consistently upregulated at the pan-cancer level, while only 15 RiboSis genes (5%) were consistently downregulated (Supplementary Figure S5, see supplementary data available online at http://bib.oxfordjournals.org/), highlighting that the changes in these RiboSis genes expression are conserved across human cancers.

To explore the RiboSis-related alterations at the DNA level, we analyzed the genetic alterations of RiboSis genes across human cancers. Overall, higher proportions of somatic copy number variations (CNVs) than single nucleotide variations (SNVs) were observed in RiboSis genes across human cancers, especially in pheochromocytoma and paraganglioma (PCPG), testicular germ cell tumors (TGCT) and uveal melanoma (UVM) (Figure 4A and B). Numerous RiboSis genes were genetically altered at high levels in different cancer types (Supplementary Figure S6A-C, see supplementary data available online at http://bib.oxfordjournals.org/). In particular, amplification of *NOP2*, *EMG1*, *DDX47*, *WBP11* and *DDX11* in TGCT (99.3% of samples; Supplementary Figure S6A, see supplementary data available online at http://bib.oxfordjournals.org/), deletion of *RPS15* in ovarian serous cystadenocarcinoma (OV) (89.3% of samples; Supplementary Figure S6B, see supplementary data available online at http://bib.oxfordjournals.org/) and deletion of *PTEN* in glioblastoma multiforme (GBM) (89.1% of samples; Supplementary Figure S6B, see supplementary data available online at http://bib.oxfordjournals.org/) were observed. These analyses revealed that the predominant somatic genetic alteration in RiboSis genes was CNV.

To gain more insight into the genomic alterations of RiboSis genes in human cancers, we then focused on CNVs, including amplifications and deletions, and assessed them based on significantly altered peaks identified by GISTIC2 ($q < 0.25$) at the pan-cancer level (Figure 4C). Interestingly, high CNV often occurred in RiboSis genes (Figure 4D) and cholangiocarcinoma (CHOL), KIRC, adrenocortical carcinoma (ACC) and PRAD showed significant amplification peak enrichments (Figure 4F). To explore potential driver events in RiboSis genes, we identified 40 recurrently amplified RiboSis genes across cancers (G-score > 0.5; Figure 4E), including *XPO1*. Together, these results suggest the essential role of recurrently amplified RiboSis genes across human cancers.

Characterization of RiboSis gene-based therapeutic targets

The dependence of tumor cells on RiboSis provides therapeutic vulnerability for cancer cells [27]. To understand the current situation of drug development of RiboSis genes, we first conducted data mining using TCRD according to the target development levels (TDLs) of RiboSis genes. Among these RiboSis genes, only two RiboSis genes (*XPO1* and *mTOR*) currently serve as therapeutic targets of FDA-approved drugs in certain cancer types (Tclin: 1%; Figure 5A), and a small portion of RiboSis genes (20/331) are targets with small molecules satisfying the activity thresholds (Tchem: 6%; Figure 5A). The majority of RiboSis genes (309, 93%) still lack corresponding compounds to manipulate their functions (77% Tbio and 16% Tdark; Figure 5A). Notably, 240 of these RiboSis genes with low target development levels (Tbio or Tdark) are essential for cancer cell growth and survival (Figure 5A). To explore whether RiboSis genes had been characterized in the previous study, we performed a publication search through PubTator. Most of the RiboSis genes (280, 85%) had not been well characterized (PubTator score < 150) and 213 of these understudied RiboSis genes are essential for cancer growth and survival (Figure 5A). Overall, a large number of insufficiently investigated RiboSis genes, which are crucial to cancer growth but lack appropriate drug interventions, provide large opportunities for further drug development.

In addition to *XPO1* and *mTOR* with approved targeting drugs, which RiboSis genes could be potential therapeutic targets? In malignant tumors, frequent alterations in genes constitute vulnerabilities for cancer treatment [44, 45], and recurrently altered genes are more likely to be potential therapeutic targets. Based on the above RiboSis-related genomic hallmarks, a total of 128 RiboSis genes were identified as potential candidates for therapeutic targets (Figure 5B). Notably, several RiboSis genes were considered potential therapeutic targets in over half of the cancer types (>16), including three RiboSis genes with recurrent amplifications, *DCAF13*, *EXOSC4* and *UTP23*. All of these three genes were more frequently amplified than *XPO1* (Figure 4E), an approved inhibitor for the treatment of relapsed or refractory multiple myeloma [46]. *TP53* was the most frequently mutated SNV hotspot at the pan-cancer level (Figure 5B; Supplementary Figure S6C, see supplementary data available online at http://bib.oxfordjournals.org/). The

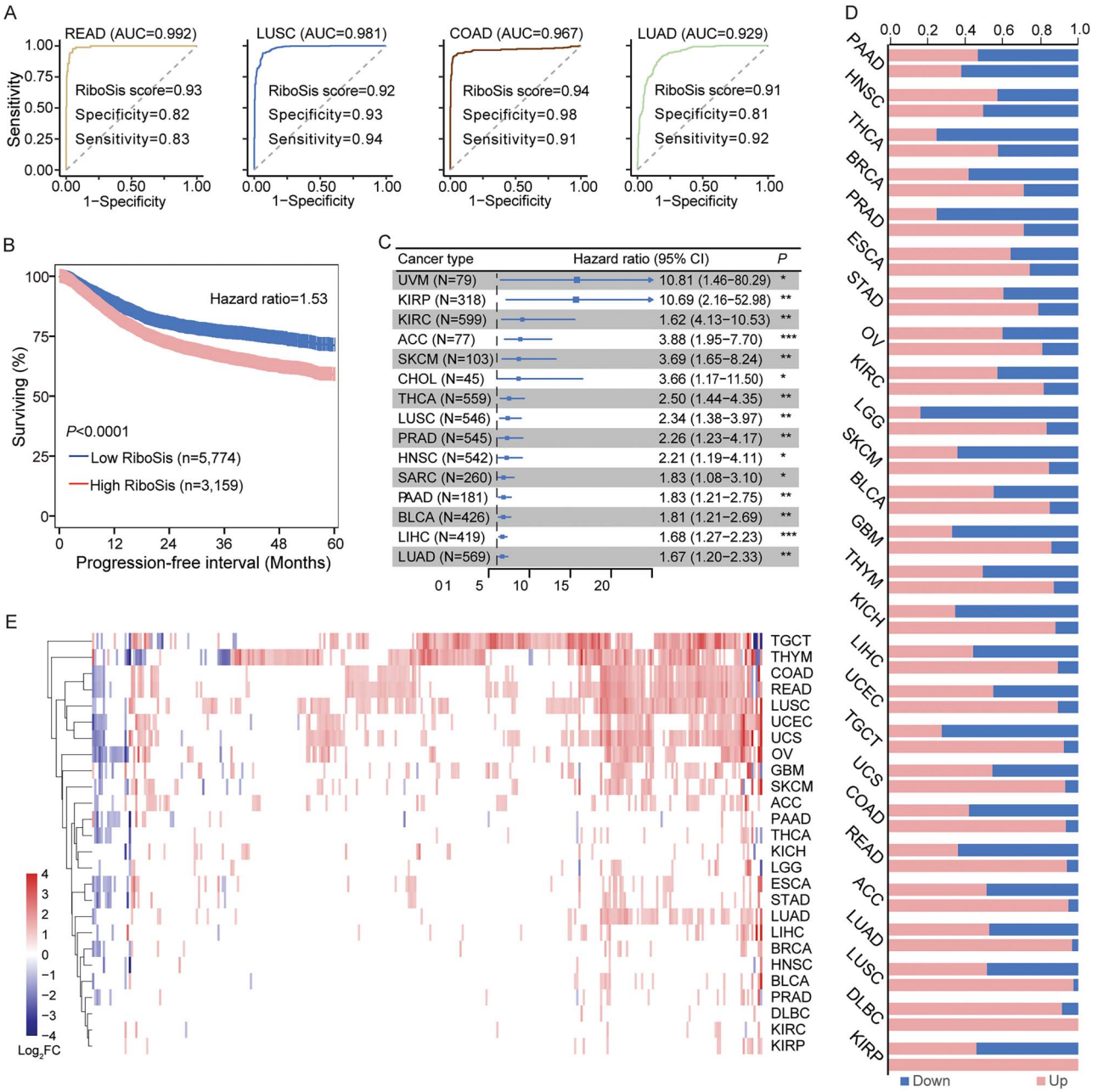

Figure 3. Upregulated ribosome biogenesis (RiboSis) genes in human cancers. (**A**) ROC curve showing the performance of RiboSis activity in distinguishing primary cancer samples from normal samples in READ, LUSC, COAD and LUAD. ROC: receiver operating characteristic; AUC: area under the ROC curve. (**B**) Progression-free interval (PFI) between primary cancer patients with high and low RiboSis activity. The number of patients is enclosed in brackets. (**C**) Hazard ratio between patients with high and low RiboSis activity across different cancer types. A Cox proportional hazards model was used to calculate the hazard ratio. The number of patients and 95% confidence interval (CI) of the hazard ratio are enclosed in brackets. (**D**) Bar diagram showing the proportion of genome-wide differentially expressed genes (up) and differentially expressed RiboSis genes (down) across 26 cancer types. (**E**) Heatmap of differentially expressed RiboSis genes across 26 cancer types. Each column represents a different RiboSis gene and each row represents a different cancer type. The shade of color represents the degree to which the expression has changed.

activity of RiboSis was significantly increased in the *TP53* missense mutation group (Figure 5C; Supplementary Figure S7, see supplementary data available online at http://bib.oxfordjournals.org/), and hyperactive RiboSis was associated with poor outcomes in LUSC patients without *TP53* mutations (Figure 5D).

By integrating transcriptome and genome data, the combined score for each of the 331 RiboSis genes was obtained using a ranking approach. Integrative analysis of the top 10 ranked genes within each cancer type revealed several hotspot genes, including *BMS1* and *XRCC5*, across multiple cancer types (Figure 5E). Collectively, our data expand the reservoir of potential RiboSis gene-based anti-tumor targets.

Putative drugs against ribosome biogenesis in cancers

Considering the long cycle of new drug development, we screened clinically approved/experimental drugs or tool compounds that may treat cancers by inhibiting RiboSis. To understand the impact of these compounds on RiboSis, we first used machine learning to

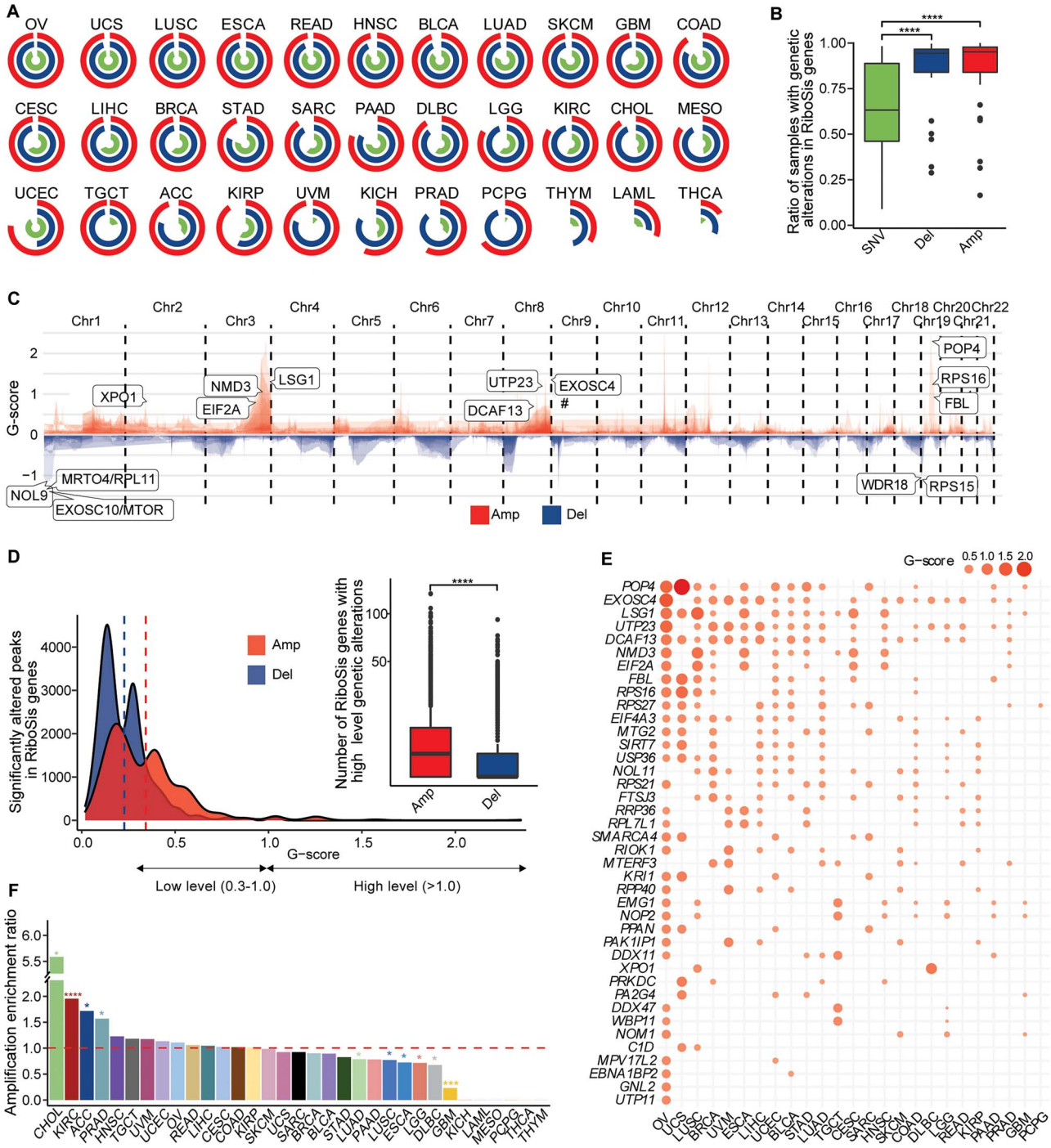

Figure 4. Characterization of somatic genetic alterations in ribosome biogenesis (RiboSis) genes. (**A**) The proportion of patients with genetic alterations in RiboSis genes across 33 cancer types. (**B**) Boxplot showing the ratio of patients with genetic alterations in RiboSis genes among SNVs, deletions and amplifications. (**C**) Area diagram showing somatic amplification and deletion on 22 autosomes at the pan-cancer level. The shade of color represents the number of cancer types, and the sites prone to alteration in more cancers are darker. The top 10 (5) RiboSis genes more likely to be amplified (deleted) are labeled. (**D**) Density plot showing the G-score of significantly altered peaks in RiboSis genes. Boxplot showing the difference in the number of RiboSis genes with high level (G-score > 1.0) genetic alterations between amplification and deletion. (**E**) Bubble diagram showing the RiboSis genes with the G-score of the top 40 across various cancer types. (**F**) Histogram showing the enrichment ratio of RiboSis genes that reside in the amplification peaks (identified by GISTIC2, q < 0.25). The enrichment ratio: fractions of RiboSis genes compared to non-RiboSis genes that reside in the amplification peaks. Significant amplification enrichments are detected with $P < 0.05$ (Fisher's exact test). ****$P < 0.0001$.

predict the drug response of 367 compounds in 9173 patients from The Cancer Genome Atlas (TCGA) cohort (Figure 6A). Combined with the expression data from TCGA, highly correlated pairs of RiboSis genes and drugs ($|r| > 0.8$, $P < 0.05$) were identified. Interestingly, RiboSis gene expression was mainly negatively related to the patient drug response, especially in DLBC and thymoma (THYM) (Figure 6B), namely, high expression of RiboSis genes was related to the increased drug sensitivity of patients. Then, we focused on the RiboSis genes whose expression exhibited a negative association with drug response for functional enrichment analysis and observed that each substep of ribosome biogenesis had an extensive correlation with target pathways of clinically

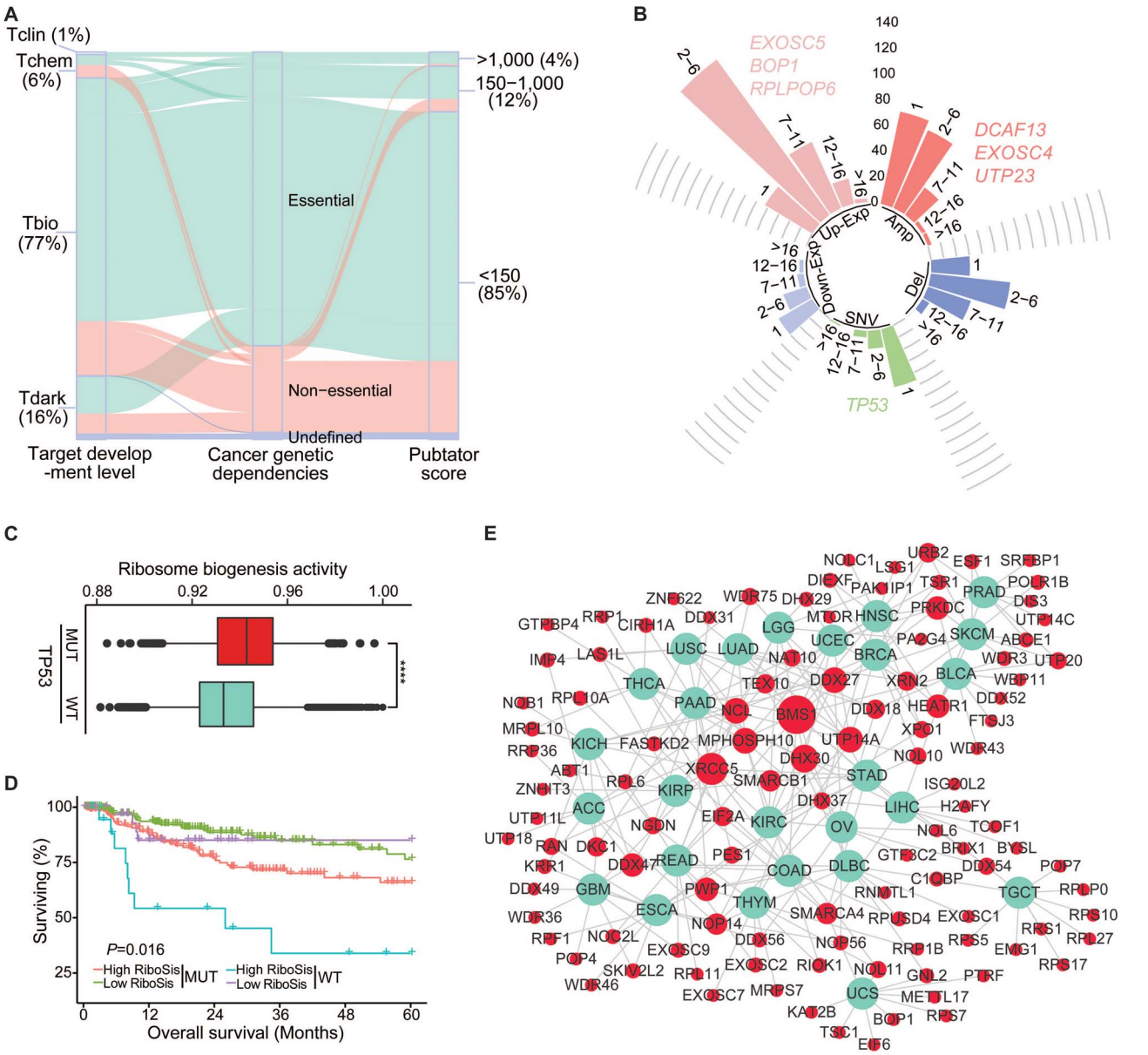

Figure 5. Characterization of ribosome biogenesis (RiboSis) gene-based therapeutic targets. (**A**) Sankey diagram showing cancer genetic dependencies of RiboSis genes based on target development level and Pubtator score. The width of the bar is proportional to the number of RiboSis genes at each corresponding level. (**B**) Bar diagram showing the number of RiboSis genes defined as potential targets in 7–11, 12–16 or > 16 cancer types at upregulated, downregulated, amplification, deletion or SNV levels. RiboSis genes defined as potential targets in more than 16 cancer types are labeled. (**C**) Boxplot showing the difference in RiboSis activity between samples with and without *TP53* mutation at the pan-cancer level. MUT: with *TP53* mutation ($n = 3248$); WT: without *TP53* mutation ($n = 5212$). ****$P < 0.0001$. (**D**) Progression-free interval (PFI) among patients with high and low RiboSis activity and with and without *TP53* mutation. (**E**) Network diagram showing the top 10 ranked RiboSis genes within each cancer type. The size of the node is scaled according to the degree of its connection.

approved/experimental drugs or tool compounds across different cancer types (Figure 6C).

Using the expression data from CCLE and the drug sensitivity data from GDSC, we then performed an association analysis between RiboSis activity and the half-maximal response of each drug. Cancer cells with higher RiboSis activity were more sensitive to 65 drugs (Figure 6D). We also performed differential drug response analysis on the activity of five substeps of RiboSis. Cancer cells with heightened activity in any of the substeps of RiboSis tended to be more sensitive to numerous drugs (Supplementary Figure S8, see supplementary data available online at http://bib.oxfordjournals.org/), and 23 drugs exhibited significant differences in drug sensitivity in all differential analyses (Figure 6E). Notably, these drugs included methotrexate, 5-fluorouracil and CX-5461, which were drugs that have been reported to possess inhibitory effects on RiboSis [28, 47], and CX-5461 shows promise in phase I trials for various malignancies [47, 48]. Thus, these data provide a valuable resource for repurposing clinically approved compounds to kill malignant cells by inhibiting RiboSis.

DISCUSSION

Despite the remarkable progress made, cancer is still a growing global health concern [49]. Various risk factors including smoking [50], chronic infection or inflammation [51–56] have been reported

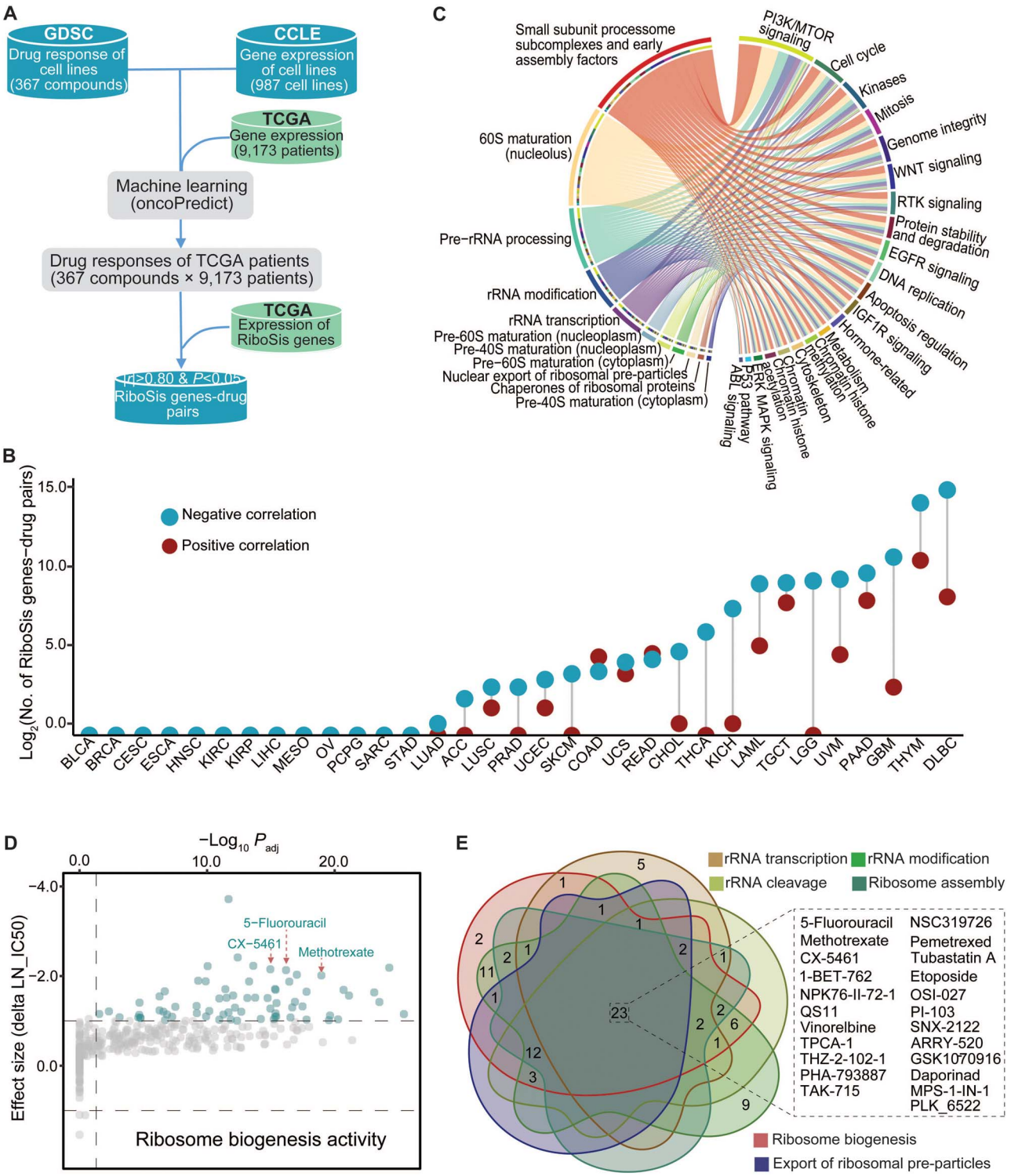

Figure 6. Putative drugs against ribosome biogenesis (RiboSis). (**A**) The workflow for identifying significant RiboSis gene-drug pairs. The drug sensitivity of patients is predicted by machine learning (oncoPredict). Combined the expression of RiboSis genes with the predicted drug sensitivity of each patient to identify significant RiboSis gene-drug pairs ($|r| > 0.8$, $P < 0.05$). (**B**) Point diagram showing the number of significant RiboSis gene-drug pairs across different cancer types. (**C**) Sankey diagram showing the enrichment result of significantly negatively correlated RiboSis genes-drug pairs. The width of the bar is proportional to the number of significantly negatively correlated RiboSis gene-drug pairs. Left: RiboSis gene enriched substeps of ribosome biogenesis; Right: drug target pathway. (**D**) Volcano plot showing the results of differential drug response analysis between cell lines with high and low RiboSis activity. Each point represents a drug. Drugs reported to be able to inhibit RiboSis are labeled. (**E**) Venn diagram showing drugs with differential drug responses in RiboSis and its five substeps. Twenty-three drugs that were identified as significantly differential drugs in all differential drug response analyses are labeled.

to be involved in the occurrence of cancer. At the molecular level, hyperactive RiboSis can prompt unrestricted growth and proliferation of cancer cells [9, 10, 57]. Unfortunately, a computational approach is still lacked to systematically evaluate the activity of RiboSis, and the hallmarks of genomic variation and therapeutic targets of RiboSis genes in human cancers are still unclear, reflecting opportunities for the development of RiboSis-based biomarkers and therapeutic strategies in oncology.

Previous studies measured the RiboSis activity using experimental approaches, such as evaluating the nucleolar size [20], silver staining of AgNOR [19], and evaluating the protein abundance [58] or rRNA abundance [22] of RNA polymerase I transcription factor. However, some of the methods are not suitable for specific cancer types [23] or are difficult to perform [24]. Here, we first defined a RiboSis gene set, and observed 76% of RiboSis genes are essential for cancer cell growth, but the majority of them are understudied (Figure 1B; Figure 5A). Next, inspired by single sample gene set enrichment analysis [26], we developed an in silico approach to calculate RiboSis activity based on the expression of the defined RiboSis gene set. In our approach, multiple RiboSis genes, instead of a single gene, were used, and the background of non-RiboSis genes of the individual transcriptome was considered to calculate the RiboSis score, which ensured the robustness of the output data. Without normalizing all samples as background, our approach and other sample-wise enrichment methods [25, 59] could directly obtain the score accurately regardless of the sample size, and characterize the heterogeneity across different cancer types. Since ribosome biogenesis is a complex biological process with other variables besides the transcript expression, it would be even better if the statistical model was used and residuals could be estimated. Although our method does not consider random variability, validation using protein expression of fibrillarin in a breast cancer cohort (Figure 1D and E, Supplementary Figure S1, see supplementary data available online at http://bib.oxfordjournals.org/) and single-cell RNA expression alteration after 5-fluorouracil treatment in colorectal cancer cells (Figure 1F) demonstrated that our developed computational approach was reliable for evaluating RiboSis activity based on transcriptome expression data. Thus, we provided a valuable resource and a reliable tool for evaluating the demand for ribosomes in the proliferation of cancer cells.

Owing to large-scale open-access data, numerous pan-cancer researches relevant to gene signatures have emerged [11–16]. However, a global blueprint of molecular alterations in all substep of RiboSis in different tumors has been lacking. Using the developed approach, we found that RiboSis was hyperactive in tumor tissues, which is consistent with experimental results in previous reports [60]. Molecular mechanism research also indicates that hyperactive RiboSis plays a central role in the development of pancreatic cancer [61], ovarian cancer [62] and colorectal cancer [63]. Interestingly, RiboSis is more active in some cancer types, such as TGCT, DLBC and rectum adenocarcinoma (READ) (Figure 2A), which may be resulted from tissue-specific ribosomal heterogeneity [64, 65]. For example, germ-cell-specific ribosome was reported to control male fertility in the testis [66]. And ribosomal heterogeneity may be related to different ribosomal modification pattern [67]. Furthermore, using single cell mRNA expression data, we revealed that the RiboSis activity of malignant cells was more active than that of other cell types in the tumor microenvironment. Thus, our results clarified that the hyperactive RiboSis in the tumor tissues was mainly due to the hyperactive RiboSis in malignant cells, providing the rationale for selectively targeting tumors over normal cells during anti-RiboSis therapy [42, 43].

It should be mentioned that the expression pattern of RiboSis was slightly different among cancers, 11 RiboSis genes, including *TP53*, were consistently up-regulated in more than half of 26 cancer types (Supplementary Figure S5, see supplementary data available online at http://bib.oxfordjournals.org/). In addition, *DDX17*, *NSUN5P1* and *PTRF* were consistently down-regulated in about half of 26 cancer types (Supplementary Figure S5, see supplementary data available online at http://bib.oxfordjournals.org/), suggesting they may have other conserved functions beyond taking part in generating ribosomes. For example, *DDX17* was reported to serve as inflammasome sensor for SINE RNAs [68], and consistently down-regulated *DDX17* may contribute to immune escape. Regarding the hallmarks of genomic alterations related to RiboSis, our multi-omic data revealed that the main genetic variation of RiboSis genes was CNV, suggesting that high-level amplification of RiboSis genes in tumors may be one of the main driving factors for hyperactive RiboSis [69, 70]. Concerted copy number variation balances are important for ribosomal DNA [71, 72]. High-level amplification of RiboSis genes might also disrupt the original genome balance [73, 74], cause conflicts [75–77], and lead to neofunctionalization [78, 79].

The demand for RiboSis in the proliferation of cancer cells provides targetable vulnerabilities for cancer therapy [27]. By integrating the pan-cancer multi-omic characteristics, we identified 128 potential therapeutic targets in RiboSis genes, including *EXOSC4* and *TP53*. *EXOSC4* is reported as a potential oncogene that is necessary for tumor cell survival [80]. *TP53* was regarded as the most frequently mutated gene at the pan-cancer level in our analysis and previous studies [81, 82], while drugs used to treat patients with or without mutations residing in the famous tumor suppressor are still on the road [83]. Interestingly, in our study, we observed that the activity of RiboSis was significantly increased in the *TP53* missense mutation group (Figure 5C; Supplementary Figure S7, see available online at http://bib.oxfordjournals.org/), and hyperactive RiboSis was associated with poor outcomes in lung squamous cell carcinoma (LUSC) patients without *TP53* mutations (Figure 5D). It has been demonstrated that impairment of RiboSis triggers redirection of the impaired ribosome biogenesis checkpoint (IRBC) complex to the binding and inhibition of *MDM2*, leading to p53 activation [22, 33, 45, 84]. It constituted a fascinating therapeutic strategy to activate the tumor suppressor function of p53 in these wild-type p53-carrying LUSC patients through blocking RiboSis, although more evidence is needed in the future studies. Additionally, we conducted a clinical correlation analysis of the RiboSis activity with clinically approved/experimental drugs, and identified 23 drugs that had inhibited RiboSis and its substeps. These drugs included known compounds inhibiting RiboSis, such as methotrexate, 5-fluorouracil and CX-5461 [28, 47]. 5-Fluorouracil can inhibit late processing of rRNA by incorporation of rRNA, CX-5461 and methotrexate are reported to inhibit rRNA transcription, and CX-5461 is showing promise in phase I trials for various malignancies [47, 48]. Although more experimental or clinical evidence for these potential targets are needed in future studies, our data expand the reservoir of potential RiboSis gene-based anti-tumor targets and provide more drugs that are likely to kill malignant cells by inhibiting RiboSis, shedding new light on RiboSis-based anti-tumor therapy.

In summary, our study presents a computational approach to systematically evaluate ribosome biogenesis activity for the first time, generates a comprehensive blueprint of molecular alterations in RiboSis genes across cancers, and provides a valuable resource for RiboSis-based anti-tumor therapy.

Key Points

- Ribosome biogenesis (RiboSis) has emerged as a new therapeutic avenue for the treatment of cancer, but a comprehensive portrait of RiboSis has been lacking to unravel novel therapeutic targets and drug candidates.
- We developed an in silico approach to quantify the activity of RiboSis and systematically characterized RiboSis activity and molecular alterations in 331 RiboSis-related genes in 33 cancer types.
- RiboSis activity was elevated in malignant cells, with high copy number amplification being the predominant mutation type.
- Patients with high RiboSis activity showed increased risk of severe outcomes in 15 cancer types including lung cancer.
- By integrating data from CCLE and GDSC, higher RiboSis activity correlated with increased sensitivity to 65 compounds, and 23 compounds ranked in high-confidence RiboSis-based anti-tumor drugs.

SUPPLEMENTARY DATA

Supplementary data are available online at http://bib.oxfordjournals.org/.

FUNDING

This work was supported by the grants from the National Natural Science Foundation of China (32370684, 32170650 and 32071156), and Beijing Natural Science Foundation (Z230007).

AUTHOR CONTRIBUTIONS STATEMENT

H.T. and Z.S. designed and supervised the study. Y.Z., X.R. and J.Y. did the bioinformatic analysis. Y.Z., X.R., J.Y., H.W., Y.W. and H.L. did clinical interpretation of molecular alterations. Y.Z., H.T. and Z.S. wrote the manuscript.

DATA AVAILABILITY

The pipeline for quantifying ribosome biogenesis activity was available via the website:https://figshare.com/articles/dataset/Pipeline_to_quantify_ribosome_biogenesis_activity/24370354.

REFERENCES

1. Shen PS, Park J, Qin Y, *et al.* Protein synthesis. Rqc2p and 60S ribosomal subunits mediate mRNA-independent elongation of nascent chains. *Science* 2015;**347**:75–8.
2. Khatter H, Myasnikov AG, Natchiar SK, Klaholz BP. Structure of the human 80S ribosome. *Nature* 2015;**520**:640–5.
3. Jiao L, Liu Y, Yu XY, *et al.* Ribosome biogenesis in disease: new players and therapeutic targets. *Signal Transduct Target Ther* 2023;**8**:15.
4. Peña C, Hurt E, Panse VG. Eukaryotic ribosome assembly, transport and quality control. *Nat Struct Mol Biol* 2017;**24**:689–99.
5. Ferreira-Cerca S, Pöll G, Gleizes PE, *et al.* Roles of eukaryotic ribosomal proteins in maturation and transport of pre-18S rRNA and ribosome function. *Mol Cell* 2005;**20**:263–75.
6. Nerurkar P, Altvater M, Gerhardy S, *et al.* Eukaryotic ribosome assembly and nuclear export. *Int Rev Cell Mol Biol* 2015;**319**:107–40.
7. Elhamamsy AR, Metge BJ, Alsheikh HA, *et al.* Ribosome biogenesis: a central player in cancer metastasis and therapeutic resistance. *Cancer Res* 2022;**82**:2344–53.
8. Zhang Z, Luo M, Li Q, *et al.* Genetic, pharmacogenomic, and immune landscapes of enhancer RNAs across human cancers. *Cancer Res* 2022;**82**:785–90.
9. Ruggero D, Pandolfi PP. Does the ribosome translate cancer? *Nat Rev Cancer* 2003;**3**:179–92.
10. Sulima SO, Hofman IJF, De Keersmaecker K, *et al.* How ribosomes translate cancer. *Cancer Discov* 2017;**7**:1069–87.
11. Jiang J, Yuan J, Hu Z, *et al.* Systematic Pan-cancer characterization of nuclear receptors identifies potential cancer biomarkers and therapeutic targets. *Cancer Res* 2022;**82**:46–59.
12. Hu Z, Yuan J, Long M, *et al.* The cancer surfaceome atlas integrates genomic, functional and drug response data to identify actionable targets. *Nat Cancer* 2021;**2**:1406–22.
13. Hu Z, Zhou J, Jiang J, *et al.* Genomic characterization of genes encoding histone acetylation modulator proteins identifies therapeutic targets for cancer treatment. *Nat Commun* 2019;**10**:733.
14. Chen C, Liu Y, Li Q, *et al.* The genetic, pharmacogenomic, and immune landscapes associated with protein expression across human cancers. *Cancer Res* 2023;**83**:3673–80.
15. Luo Z, Liu W, Sun P, *et al.* Pan-cancer analyses reveal regulation and clinical outcome association of the shelterin complex in cancer. *Brief Bioinform* 2021;**22**:bbaa441.
16. Wang J, Dai M, Xing X, *et al.* Genomic, epigenomic, and transcriptomic signatures for telomerase complex components: a pan-cancer analysis. *Mol Oncol* 2023;**17**:150–72.
17. Catez F, Dalla Venezia N, Marcel V, *et al.* Ribosome biogenesis: an emerging druggable pathway for cancer therapeutics. *Biochem Pharmacol* 2019;**159**:74–81.
18. Hald ØH, Olsen L, Gallo-Oller G, *et al.* Inhibitors of ribosome biogenesis repress the growth of MYCN-amplified neuroblastoma. *Oncogene* 2019;**38**:2800–13.
19. Teixeira G, Antonangelo L, Kowalski L, *et al.* Argyrophilic nucleolar organizer regions staining is useful in predicting recurrence-free interval in oral tongue and floor of mouth squamous cell carcinoma. *Am J Surg* 1996;**172**:684–8.
20. Xu J, Zhong A, Zhang S, *et al.* KMT2D deficiency promotes myeloid leukemias which is vulnerable to ribosome biogenesis inhibition. *Adv Sci (Weinh)* 2023;**10**:e2206098.
21. Marcel V, Ghayad SE, Belin S, *et al.* p53 acts as a safeguard of translational control by regulating fibrillarin and rRNA methylation in cancer. *Cancer Cell* 2013;**24**:318–30.
22. Bywater MJ, Poortinga G, Sanij E, *et al.* Inhibition of RNA polymerase I as a therapeutic strategy to promote cancer-specific activation of p53. *Cancer Cell* 2012;**22**:51–65.
23. Penzo M, Montanaro L, Treré D, Derenzini M. The ribosome biogenesis-cancer connection. *Cell* 2019;**8**:8.
24. Stamatopoulou V, Parisot P, De Vleeschouwer C, *et al.* Use of the iNo score to discriminate normal from altered nucleolar morphology, with applications in basic cell biology and potential in human disease diagnostics. *Nat Protoc* 2018;**13**:2387–406.
25. Foroutan M, Bhuva DD, Lyu R, *et al.* Single sample scoring of molecular phenotypes. *BMC Bioinformatics* 2018;**19**:404.
26. Hänzelmann S, Castelo R, Guinney J. GSVA: gene set variation analysis for microarray and RNA-seq data. *BMC Bioinformatics* 2013;**14**:7.

27. Pelletier J, Thomas G, Volarević S. Ribosome biogenesis in cancer: new players and therapeutic avenues. *Nat Rev Cancer* 2018;**18**: 51–63.
28. Burger K, Mühl B, Harasim T, *et al.* Chemotherapeutic drugs inhibit ribosome biogenesis at various levels. *J Biol Chem* 2010;**285**:12416–25.
29. Ghoshal K, Jacob ST. Specific inhibition of pre-ribosomal RNA processing in extracts from the lymphosarcoma cells treated with 5-fluorouracil. *Cancer Res* 1994;**54**:632–6.
30. Trask DK, Muller MT. Stabilization of type I topoisomerase-DNA covalent complexes by actinomycin D. *Proc Natl Acad Sci U S A* 1988;**85**:1417–21.
31. Bruno PM, Liu Y, Park GY, *et al.* A subset of platinum-containing chemotherapeutic agents kills cells by inducing ribosome biogenesis stress. *Nat Med* 2017;**23**:461–71.
32. Kim DS, Camacho CV, Nagari A, *et al.* Activation of PARP-1 by snoRNAs controls ribosome biogenesis and cell growth via the RNA helicase DDX21. *Mol Cell* 2019;**75**:1270–1285.e14.
33. Kang J, Brajanovski N, Chan KT, *et al.* Ribosomal proteins and human diseases: molecular mechanisms and targeted therapy. *Signal Transduct Target Ther* 2021;**6**:323.
34. Love MI, Huber W, Anders S. Moderated estimation of fold change and dispersion for RNA-seq data with DESeq2. *Genome Biol* 2014;**15**:550.
35. Mermel CH, Schumacher SE, Hill B, *et al.* GISTIC2.0 facilitates sensitive and confident localization of the targets of focal somatic copy-number alteration in human cancers. *Genome Biol* 2011;**12**:R41.
36. Maeser D, Gruener RF, Huang RS. oncoPredict: an R package for predicting in vivo or cancer patient drug response and biomarkers from cell line screening data. *Brief Bioinform* 2021;**22**:bbab260.
37. Pacini C, Dempster JM, Boyle I, *et al.* Integrated cross-study datasets of genetic dependencies in cancer. *Nat Commun* 2021;**12**:1661.
38. Yoshikawa H, Ishikawa H, Izumikawa K, *et al.* Human nucleolar protein Nop52 (RRP1/NNP-1) is involved in site 2 cleavage in internal transcribed spacer 1 of pre-rRNAs at early stages of ribosome biogenesis. *Nucleic Acids Res* 2015;**43**:5524–36.
39. Therizols G, Bash-Imam Z, Panthu B, *et al.* Alteration of ribosome function upon 5-fluorouracil treatment favors cancer cell drug-tolerance. *Nat Commun* 2022;**13**:173.
40. Chalabi-Dchar M, Fenouil T, Machon C, *et al.* A novel view on an old drug, 5-fluorouracil: an unexpected RNA modifier with intriguing impact on cancer cell fate. *NAR Cancer* 2021;**3**:zcab032.
41. Park SR, Namkoong S, Friesen L, *et al.* Single-cell transcriptome analysis of colon cancer cell response to 5-fluorouracil-induced DNA damage. *Cell Rep* 2020;**32**:108077.
42. Drygin D, Lin A, Bliesath J, *et al.* Targeting RNA polymerase I with an oral small molecule CX-5461 inhibits ribosomal RNA synthesis and solid tumor growth. *Cancer Res* 2011;**71**:1418–30.
43. Hein N, Hannan KM, George AJ, *et al.* The nucleolus: an emerging target for cancer therapy. *Trends Mol Med* 2013;**19**:643–54.
44. Chen C, Han L. Multi-omic genetic scores advance disease research. *Trends Genet* 2023;**39**:600–1.
45. Bursać S, Prodan Y, Pullen N, *et al.* Dysregulated ribosome biogenesis reveals therapeutic liabilities in cancer. *Trends Cancer* 2021;**7**:57–76.
46. Syed YY. Selinexor: first global approval. *Drugs* 2019;**79**:1485–94.
47. Mars JC, Tremblay MG, Valere M, *et al.* The chemotherapeutic agent CX-5461 irreversibly blocks RNA polymerase I initiation and promoter release to cause nucleolar disruption, DNA damage and cell inviability, NAR. *Cancer* 2020;**2**:zcaa032.
48. Khot A, Brajanovski N, Cameron DP, *et al.* First-in-human RNA polymerase I transcription inhibitor CX-5461 in patients with advanced hematologic cancers: results of a phase I dose-escalation study. *Cancer Discov* 2019;**9**:1036–49.
49. Siegel RL, Miller KD, Wagle NS, Jemal A. Cancer statistics, 2023. *CA Cancer J Clin* 2023;**73**:17–48.
50. Malhotra J, Malvezzi M, Negri E, *et al.* Risk factors for lung cancer worldwide. *Eur Respir J* 2016;**48**:889–902.
51. Arthur JC, Perez-Chanona E, Muhlbauer M, *et al.* Intestinal inflammation targets cancer-inducing activity of the microbiota. *Science* 2012;**338**:120–3.
52. Khan S. Potential role of *Escherichia coli* DNA mismatch repair proteins in colon cancer. *Crit Rev Oncol Hematol* 2015;**96**:475–82.
53. Khan S, Zakariah M, Rolfo C, *et al.* Prediction of mycoplasma hominis proteins targeting in mitochondria and cytoplasm of host cells and their implication in prostate cancer etiology. *Oncotarget* 2017;**8**:30830–43.
54. Khan S, Zakariah M, Palaniappan S. Computational prediction of mycoplasma hominis proteins targeting in nucleus of host cell and their implication in prostate cancer etiology. *Tumour Biol* 2016;**37**:10805–13.
55. Khan S, Imran A, Khan AA, *et al.* Systems biology approaches for the prediction of possible role of chlamydia pneumoniae proteins in the etiology of lung cancer. *PloS One* 2016;**11**:e0148530.
56. Wang Y, Imran A, Shami A, *et al.* Decipher the helicobacter pylori protein targeting in the nucleus of host cell and their implications in gallbladder cancer: an insilico approach. *J Cancer* 2021;**12**:7214–22.
57. Wiecek AJ, Cutty SJ, Kornai D, *et al.* Genomic hallmarks and therapeutic implications of G0 cell cycle arrest in cancer. *Genome Biol* 2023;**24**:128.
58. Bianco C, Mohr I. Ribosome biogenesis restricts innate immune responses to virus infection and DNA. *Elife* 2019;**8**:8.
59. Bhuva DD, Cursons J, Davis MJ. Stable gene expression for normalisation and single-sample scoring. *Nucleic Acids Res* 2020;**48**:e113.
60. Montanaro L, Trere D, Derenzini M. Nucleolus, ribosomes, and cancer. *Am J Pathol* 2008;**173**:301–10.
61. Antal CE, Oh TG, Aigner S, *et al.* A super-enhancer-regulated RNA-binding protein cascade drives pancreatic cancer. *Nat Commun* 2023;**14**:5195.
62. Hao Q, Li J, Zhang Q, *et al.* Single-cell transcriptomes reveal heterogeneity of high-grade serous ovarian carcinoma. *Clin Transl Med* 2021;**11**:e500.
63. Dong Z, Li J, Dai W, *et al.* RRP15 deficiency induces ribosome stress to inhibit colorectal cancer proliferation and metastasis via LZTS2-mediated beta-catenin suppression. *Cell Death Dis* 2023;**14**:89.
64. Genuth NR, Barna M. The discovery of ribosome heterogeneity and its implications for gene regulation and organismal life. *Mol Cell* 2018;**71**:364–74.
65. Simsek D, Tiu GC, Flynn RA, *et al.* The mammalian Ribo-interactome reveals ribosome functional diversity and heterogeneity. *Cell* 2017;**169**:1051–1065.e18.
66. Li H, Huo Y, He X, *et al.* A male germ-cell-specific ribosome controls male fertility. *Nature* 2022;**612**:725–31.
67. Krogh N, Asmar F, Come C, *et al.* Profiling of ribose methylations in ribosomal RNA from diffuse large B-cell lymphoma patients for evaluation of ribosomes as drug targets. *NAR Cancer* 2020;**2**:zcaa035.
68. Fortuna TR, Kour S, Anderson EN, *et al.* DDX17 is involved in DNA damage repair and modifies FUS toxicity in an RGG-domain dependent manner. *Acta Neuropathol* 2021;**142**:515–36.

69. Cui K, Gong L, Zhang H, *et al.* EXOSC8 promotes colorectal cancer tumorigenesis via regulating ribosome biogenesis-related processes. *Oncogene* 2022;**41**:5397–410.
70. Cui K, Liu C, Li X, *et al.* Comprehensive characterization of the rRNA metabolism-related genes in human cancer. *Oncogene* 2020;**39**:786–800.
71. Gibbons JG, Branco AT, Godinho SA, *et al.* Concerted copy number variation balances ribosomal DNA dosage in human and mouse genomes. *Proc Natl Acad Sci U S A* 2015;**112**:2485–90.
72. Malone JH. Balancing copy number in ribosomal DNA. *Proc Natl Acad Sci U S A* 2015;**112**:2635–6.
73. Drews RM, Hernando B, Tarabichi M, *et al.* A pan-cancer compendium of chromosomal instability. *Nature* 2022;**606**: 976–83.
74. Steele CD, Abbasi A, Islam SMA, *et al.* Signatures of copy number alterations in human cancer. *Nature* 2022;**606**:984–91.
75. Wang M, Lemos B. Ribosomal DNA copy number amplification and loss in human cancers is linked to tumor genetic context, nucleolus activity, and proliferation. *PLoS Genet* 2017;**13**:e1006994.
76. Garcia-Muse T, Aguilera A. Transcription-replication conflicts: how they occur and how they are resolved. *Nat Rev Mol Cell Biol* 2016;**17**:553–63.
77. Hamperl S, Cimprich KA. Conflict resolution in the genome: how transcription and replication make it work. *Cell* 2016;**167**: 1455–67.
78. Bayer A, Brennan G, Geballe AP. Adaptation by copy number variation in monopartite viruses. *Curr Opin Virol* 2018;**33**:7–12.
79. Bhattacharya A, Bense RD, Urzua-Traslavina CG, *et al.* Transcriptional effects of copy number alterations in a large set of human cancers. *Nat Commun* 2020;**11**:715.
80. Pan Y, Tong JHM, Kang W, *et al.* EXOSC4 functions as a potential oncogene in development and progression of colorectal cancer. *Mol Carcinog* 2018;**57**:1780–91.
81. Rivlin N, Brosh R, Oren M, Rotter V. Mutations in the p53 tumor suppressor gene: important milestones at the various steps of tumorigenesis. *Genes Cancer* 2011;**2**:466–74.
82. Rheinbay E, Nielsen MM, Abascal F, *et al.* Analyses of non-coding somatic drivers in 2,658 cancer whole genomes. *Nature* 2020;**578**: 102–11.
83. Hsiue EH, Wright KM, Douglass J, *et al.* Targeting a neoantigen derived from a common *TP53* mutation. *Science* 2021;**371**:eabc8697.
84. Nishimura K, Kumazawa T, Kuroda T, *et al.* Perturbation of ribosome biogenesis drives cells into senescence through 5S RNP-mediated p53 activation. *Cell Rep* 2015;**10**:1310–23.